J. Astrophys. Astr. (2014) **35,** 607–618

Lunar-Forming Giant Impact Model Utilizing Modern Graphics Processing Units

J. C. Eiland[1], T. C. Salzillo[1], B. H. Hokr[2], J. L. Highland[2], W. D. Mayfield[1] & B. M. Wyatt[1,*]

[1]*Department of Mathematics, Tarleton State University, Stephenville, TX 76402, USA.*
[2]*Department of Physics and Astronomy, Texas A&M University, College Station, TX 77843, USA.*
[*]*e-mail: wyatt@tarleton.edu*

Received 28 January 2014; accepted 30 May 2014

Abstract. Recent giant impact models focus on producing a circumplanetary disk of the proper composition around the Earth and defer to earlier works for the accretion of this disk into the Moon. The discontinuity between creating the circumplanetary disk and accretion of the Moon is unnatural and lacks simplicity. In addition, current giant impact theories are being questioned due to their inability to find conditions that will produce a system with both the proper angular momentum and a resultant Moon that is isotopically similar to the Earth. Here we return to first principles and produce a continuous model that can be used to rapidly search the vast impact parameter space to identify plausible initial conditions. This is accomplished by focusing on the three major components of planetary collisions: constant gravitational attraction, short range repulsion and energy transfer. The structure of this model makes it easily parallelizable and well-suited to harness the power of modern Graphics Processing Units (GPUs). The model makes clear the physically relevant processes, and allows a physical picture to naturally develop. We conclude by demonstrating how the model readily produces stable Earth–Moon systems from a single, continuous simulation. The resultant systems possess many desired characteristics such as an iron-deficient, heterogeneously-mixed Moon and accurate axial tilt of the Earth.

Key words. Accretion: accretion disks—Earth—Moon—planets and satellites: formation.

1. Introduction

Prior to landing on the Moon, three theories dominated the debates on the origins of the Moon. First, could the Moon be a twin planet to Earth formed out of the same cloud of gas and dust? If so, their overall compositions would be very similar

(Stevenson 1987; Newsom & Taylor 1989; Schneider & Arny 2012). However, the Moon has a relatively small proportion of iron when compared to Earth, so this is unlikely. Second, is the Moon a captured rocky planet? If this were true, the Moon's composition would probably be unlike Earth's. Yet the Moon has striking similarities to the Earth in several isotopes (Wiechert *et al.* 2001; Touboul *et al.* 2007; Halliday 2012; Meier 2012; Zhang *et al.* 2012), so this is also unlikely. Third, could a young, fast-spinning Earth have spun off a large section of its mantle to form the Moon? This would explain the Moon's iron deficiency and similarities to Earth's mantle (Ringwood 1962). However, the Moon's absence of volatiles suggests that it originated in a hotter environment than the Earth (Newsom & Taylor 1989), leaving this fission theory flawed.

The origin of Earth's Moon continues to be a heavily debated topic in planetary science today. How could the Moon have many similar isotopic ratios to Earth, yet have a shortage of volatiles and lack a large amount of iron (Schneider & Arny 2012)? In 1975, Hartmann and Davis, and then independently in 1976, Cameron and Ward proposed the giant impact hypothesis to answer this question (Hartmann & Davis 1975; Cameron & Ward 1976; Stevenson 1987). The hypothesis states that the Earth–Moon system was formed by the collision of the early Earth and a Mars-sized planet named Theia. Their heavy iron cores coalesced, and a large amount of crust and mantle material was violently ejected, leaving the system in a state of high angular momentum. The ejected material is thought to have created a circumplanetary disk around the Earth which later accreted to become the Moon (Benz *et al.* 1986; Palme 2004). Computer simulations added credibility to this theory by numerically demonstrating that Moon formation from a giant impact was feasible (Stevenson 1987; Ida *et al.* 1997; Canup & Asphaug 2001). Most numerical simulations of this theory focus on creating a disk of debris with the appropriate mass and composition which could lead to the formation of the Moon (Canup 2003; Canup 2012; Cuk & Stewart 2012; Reufer *et al.* 2012). Other simulations start with a disk of debris and demonstrate how this disk can coalesce into the Moon (Ida *et al.* 1997; Kokubo *et al.* 2000). This discontinuous two-part simulation scheme lacks cohesion and makes resultant Moon-forming models seem contrived. In addition, many aspects of lunar-forming impacts are difficult to study with a two-part simulation, such as how impactor initial conditions affect the axial tilt and rotation of the resultant Moon.

Here we describe a model that exhibits continuity between a giant impact and Moon formation. The model readily produces, in a single simulation, an iron-deficient Moon that is isotopically similar to the Earth, and an Earth whose equatorial plane is properly tilted off the ecliptic plane. Additionally, the structure of the model is such that it can easily be optimized to run on a low cost Graphics Processing Unit (GPU). This was accomplished by focusing on the three major components of planetary interactions: the weak but ever present attractive force of gravity, the strong but short-ranged repulsive force during physical contact, and the energy loss during collisions due to heating and deformation. This allowed the functions of interaction to be simply structured so that they could be efficiently parallelized for distribution of work to the massive number of processors available on modern graphics cards. The model coupled with the compute capability of the GPU enables rapid testing of collision scenarios in the search for promising initial conditions.

2. Methodology

In this work, large aggregates of spheres with identical radii, referred to as elements, are grouped together to form bodies, referred to as impactors. The dynamics of the model are solely determined by the sum of all pairwise forces between elements. These pairwise forces are described as follows. When two elements are not in physical contact, they interact solely through the attractive force of gravity. While in physical contact the elements experience a repulsive force. The contact region of two overlapping spheres is a circle with an area determined by the separation of their centers. Thus, this repulsive force is proportional to the square of the separation between elements (Mravlak 2008). To simulate an element's resistance to deformation, each is given a shell. If this shell is not penetrated, the repulsive force is elastic. If the shell is penetrated, the force is inelastic to account for energy transferred into heat, as well as deformation of the element. As two elements converge past their shell depths, the repulsion force remains strong, but as they separate, this repulsive force is greatly reduced until the elements are no longer in contact. In short the repulsion force at low energies is elastic while at high energies it is inelastic to model deformation and energy transfer. Each impactor is composed of two types of elements: silicate material and iron (Canup 2012). Silicate and iron elements are allowed to have different repulsive strengths, different repulsion reductions, and different shell depths. For the purpose of this explanation, it is assumed that the shell depth of iron is greater than that of the silicate, but this is not a necessary condition. The force interaction between a silicate and an iron element are presented in Fig. 1 and Tables 1 and 2.

A check to see if the separation between two elements is less than epsilon must be performed because of the singularity in the gravitational force. If the separation between elements becomes too small, it is an indication that the repulsive parameters are not set strong enough. When this occurred, it was recorded and the simulation was terminated. Interactions between two iron elements or two silicate elements are described in a similar manner.

Approximating gravity can cause models to behave unnaturally. Hence, to remove all uncertainty in this area, we choose to run a full N-squared model where gravity is not approximated. The tolerance for the minimum separation, epsilon, was set to be the distance that maximized the repulsive force of the element–element interaction. This selection was chosen because the singularity of gravity causes a decrease in the repulsive force past this point, which is unnatural. Because there are three such cases, iron–iron interactions, silicate–silicate interactions, and iron–silicate interactions, epsilon was chosen to be the largest value over all three cases. The repulsive parameters were set so that the impactors could withstand a high velocity head on

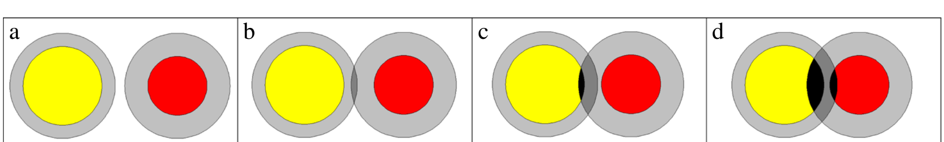

Figure 1. Different element–element force situations. The silicate element is yellow with a grey shell. The iron element is red with a grey shell. (**a**) Elements are not in contact, **(b)** elements are in contact but neither shell is penetrated, **(c)** silicate shell has been penetrated, but not the iron shell, **(d)** both shells have been penetrated.

Table 1. Force function parameters.

Parameter	Description
r	Separation between element centers
D	Diameter of an element[a]
M_{Si}	Mass of a silicate element
M_{Fe}	Mass of an iron element
K_{Si}	Repulsive parameter for silicate
K_{Fe}	Repulsive parameter for iron
KRP_{Si}	Per cent of reduction of the silicate repulsive force
KRP_{Fe}	Per cent of reduction of the iron repulsive force
SDP_{Si}	Shell depth per cent of diameter of a silicate element
SDP_{Fe}	Shell depth per cent of diameter of an iron element
G	Universal gravitational constant
Epsilon	Minimum separation allowed

Notes. [a]Iron and silicate elements have a common diameter.

impact without the model losing integrity by having element–element separations decreasing past epsilon. Repulsion parameters were also adjusted so that elements in the core would not appreciably overlap in low energy situations. This would have changed the effective densities set for the elements. Shell depths were set so that energy loss would be minimal when the bodies were not under significant stress. The shells were also needed to prevent undesired energy loss due to the small element–element vibrations caused by numeric integration through time. Repulsion reduction parameters were adjusted to produce satellites from the impact. If the repulsion reduction parameters are set too low, ejected elements will not coalesce to produce satellites. If the repulsion reduction parameters are set too high, the amount of ejected material is too low to produce large satellites. The selections were done through an iterative process because of the complex interrelations between the various model parameters.

Following the lead of Robin Canup of the Southwest Research Institute, each impactor had approximately the same size and composition as present day Earth (Canup 2012). Of the elements that formed each impactor, 70 per cent of the mass was from elements with a silicate material density, and 30 per cent of the mass was from elements with an iron density. Incorporating the work done by Matija Cuk and Sarah Stewart of Harvard, the impactors were given large angular velocities of just

Table 2. Force function.

Element–element separation	Force if separation is decreasing	Force if separation is increasing
$D \le r$ (see Figure 1a)	$G \cdot M_{Si} \cdot M_{Fe} \cdot r^{-2}$	Same as decreasing separation
$D - D \cdot SDP_{Si} \le r < D$ (see Figure 1b)	$G \cdot M_{Si} \cdot M_{Fe} \cdot r^{-2} - 0.5 \cdot (K_{Si} + K_{Fe})(D^2 - r^2)$	Same as decreasing separation
$D - D \cdot SDP_{Fe} \le r < D - D \cdot SDP_{Si}$ (see Figure 1c)	$G \cdot M_{Si} \cdot M_{Fe} \cdot r^{-2} - 0.5 \cdot (K_{Si} + K_{Fe})(D^2 - r^2)$	$G \cdot M_{Si} \cdot M_{Fe} \cdot r^{-2} - 0.5 \cdot (K_{Si} \cdot KRP_{Si} + K_{Fe})(D^2 - r^2)$
Epsilon $\le r < D - D \cdot SDP_{Fe}$ (see Figure 1d)	$G \cdot M_{Si} \cdot M_{Fe} \cdot r^{-2} - 0.5 \cdot (K_{Si} + K_{Fe})(D^2 - r^2)$	$G \cdot M_{Si} \cdot M_{Fe} \cdot r^{-2} - 0.5 \cdot (K_{Si} \cdot KRP_{Si} + K_{Fe} \cdot KRP_{Fe})(D^2 - r^2)$
$r <$ epsilon	Set r equal to epsilon and calculate accordingly	Same as decreasing separation

over a 2-hour period (Cuk & Stewart 2012). We deviate from these models in that we use a much smaller linear impact velocity. The examples presented in this work use relative closing velocities 7.7 to 3.1 times slower than those presented in the paper of Cuk & Stewart (2012). This is justified because both impactors are believed to have been rocky planets which would have formed inside the asteroid belt. In addition, their orbits around the Sun would have been similar causing an impact velocity slower than the escape velocity of the Earth which is commonly used.

3. Additional background

The present-day Moon orbits the Earth with an eccentricity of 0.055 and an average distance from the Earth of about 60 Earth radii (Backman & Seeds 2010). The Moon's orbit is tidally coupled with the Earth, meaning its orbital period and rotational period are equal. This is why we only see one side of the Moon. Tidal forces between the Earth and the Moon created this synchronization and are still at work today by adjusting the system. Angular momentum is being transferred from the Earth to the Moon, causing Earth's rotation to slow and the orbital speed of the Moon to increase (Cuk & Stewart 2012). It is believed that the Moon accreted just outside the Earth's Roche radius which is approximately 2.9 times the Earth's radius (Ida *et al.* 1997). A Moon can only form outside the Roche radius since satellites held together solely by gravity will be torn apart by the Earth's tidal forces inside this region (Cuk & Stewart 2012). The radius of the Earth is approximately 3.7 times that of the Moon. The mass of the Earth is approximately 81 times that of the Moon. Earth's equatorial plane is tilted 23.4 degrees off the ecliptic plane (Backman & Seeds 2010). Outside of small deviations due to nutation, this angle remains constant with respect to the ecliptic plane and precesses with a period of 26,000 years (Whipple 1981).

4. Simulations

Three examples of simulations generated by the model are presented here. The first, a planar single-tailed collision, demonstrates how the model produces a stable Earth–Moon system from a giant impact in which the angular momentum can be controlled. The second, a planar double-tailed collision, demonstrates production of a Moon composed of almost equal amounts of material from each impactor. The third example preserves the characteristics of the second simulation but introduces an off-planar collision which produces an Earth whose equatorial plane is tilted off the ecliptic plane within two degrees of the observed value.

4.1 *Planar single-tailed collision*

Most objects in our solar system reside in the ecliptic plane and orbit the Sun in the same direction (Feynman *et al.* 2006; Schneider & Arny 2012). Hence a natural scenario could be that two young, rapidly spinning proto-planets, rotating and orbiting together in the ecliptic plane, would have collided. The simulation depicted here is of an off-centered collision of two impactors with large opposite angular velocities, both rotating in the ecliptic plane. Because the impactors spun in opposite directions, one impactor spun into the collision, while the other spun out of the collision. This

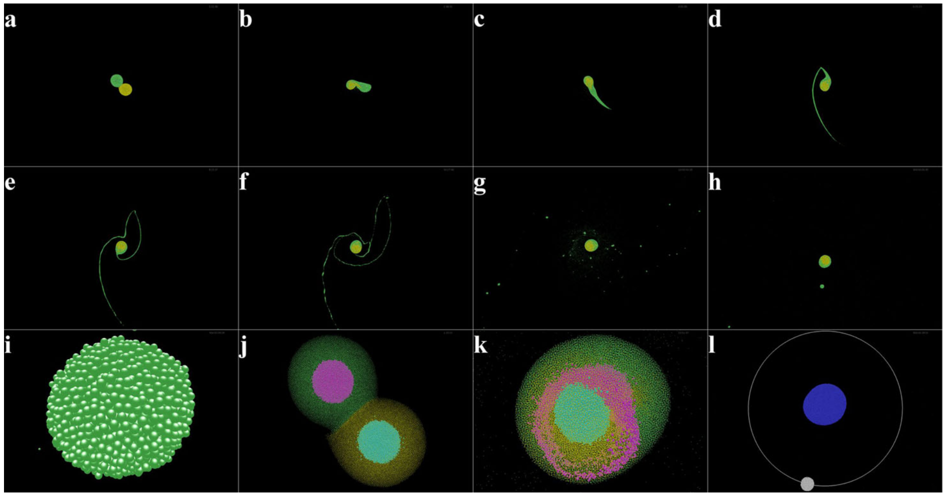

Figure 2. Planar single-tailed collision (131,072 elements). **(a–h)** Top view of collision at 1.20, 2.65, 4.03, 6.48, 8.43, 10.47, 24.00 and 720.00 hours, respectively, into the simulation. The green impactor is spinning clockwise. The yellow impactor is spinning counter clockwise. **(i)** Close up of the resultant Moon. **(j)** View of impactor cores at the point of impact. Green and yellow are silicate elements. Cyan and magenta are iron elements. **(k)** View of the resultant Earth's core. **(l)** Trace of the resultant Moon's orbit.

caused a single-tailed spiral with the tail being composed solely of elements from the impactor spinning out of the collision (see Figure 2).

The simulation ran for 720 simulated hours with the following results. A dominant Moon 1/30 the mass of the resultant Earth was formed. The Moon was composed predominantly of silicate material. The Earth day was 4.20 hours. The orbital period of the Moon around the Earth was 18.39 hours. The average distance from the centre of the Earth to the centre of the Moon was 44,224 km. The eccentricity of the Moon's orbit was 0.078. Figure 2l shows that the Moon formed just past the Roche limit. Since the impactors were rotating in opposite directions, the total angular momentum of the system could be controlled, but the resultant Moon was composed

Table 3. Parameters for planar single-tailed collision.

Parameter	Value
D	376.78 km
M_{Si}	$7.4161 \cdot 10^{19}$ kg
M_{Fe}	$1.9549 \cdot 10^{20}$ kg
K_{Si}	$2.9114 \cdot 10^{11}$kg m^{-1} s^{-2}
K_{Fe}	$5.8228 \cdot 10^{11}$kg m^{-1} s^{-2}
KRP_{Si}	0.01
KRP_{Fe}	0.02
SDP_{Si}	0.001
SDP_{Fe}	0.002
Epsilon	47.0975 km
Time step	5.8117 s
Numerical technique	Leap-frog formulas

Table 4. Initial values for planar single-tailed collision–yellow impactor.

Parameter	x value	y value	z value
Center of mass	23925.0 km	0.0 km	9042.7 km
Linear velocity	-3.2416 km s^{-1}	0.0 km s^{-1}	0.0 km s^{-1}
Angular velocity	0.0 rad h^{-1}	3.0973 rad h^{-1}	0.0 rad h^{-1}

Table 5. Initial values for planar single-tailed collision–green impactor.

Parameter	x value	y value	z value
Center of mass	-23925.0 km	0.0 km	-9042.7 km
Linear velocity	3.2416 km s^{-1}	0.0 km s^{-1}	0.0 km s^{-1}
Angular velocity	0.0 rad h^{-1}	-3.0973 rad h^{-1}	0.0 rad h^{-1}

predominantly of material from the impactor spinning out of collision. The initial parameters used for this simulation are provided in Tables 3–5.

4.2 *Planar double-tailed collision*

With the exception of Venus and Uranus, planets in our solar system not only orbit the Sun in the same direction, but also spin on their axes in the same direction (Feynman *et al.* 2006; Schneider & Arny 2012). Therefore, a more likely scenario than the one producing the planar single-tailed collision is that of an off-centred collision of two young proto-planets, both orbiting and spinning in the same direction in the ecliptic plane. Simulations of same-sized impactors where both impactors spun into the collision produced no spiral of debris, and consequently no large satellites

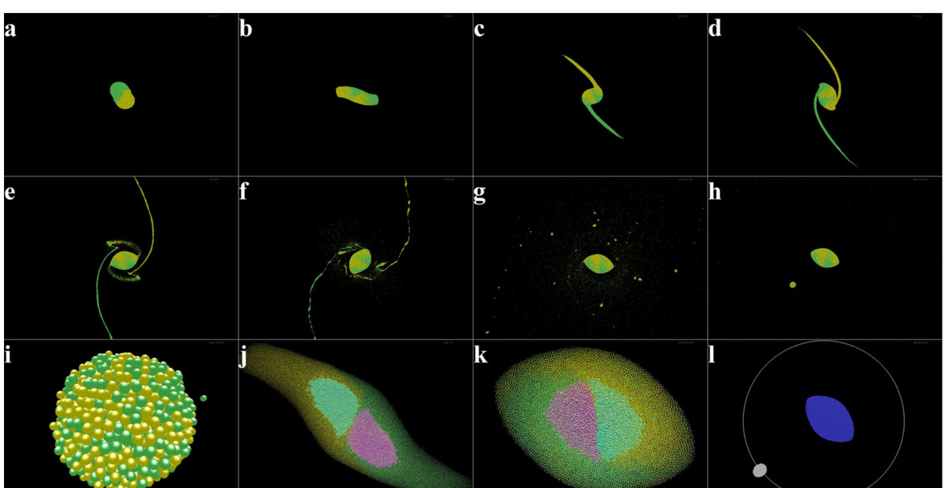

Figure 3. Planar double-tailed collision (131,072 elements). **(a–h)** Top view of collision at 4.23, 5.27, 6.75, 7.88, 10.40, 13.33, 24.00, and 720.00 hours, respectively, into the simulation. Both impactors are spinning clockwise. **(i)** Close up of the resultant Moon. **(j)** View of impactor cores during impact. **(k)** View of the resultant Earth's core. **(l)** Trace of resultant Moon's orbit.

were formed. However, simulations with both impactors spinning out of the collision produced a double-tailed spiral, one spiral being composed of elements from one impactor, and the other spiral being composed of elements from the second impactor (see Figure 3).

The simulation ran for 720 simulated hours with the following results. A dominant Moon 1/45 the mass of the resultant Earth was formed. The Moon was composed predominantly of silicate material. The Moon was composed of almost equal amounts of material from each impactor, 48.8 % from the yellow impactor and the remaining 51.2 % from the green impactor. The Earth day was 3.39 hours. The orbital period of the Moon around the Earth was 17.91 hours. The average distance from the centre of the Earth to the centre of the Moon was 43,391 km. The eccentricity of the orbit was 0.077. This simulation possesses most of the qualities of the last simulation with the addition of a heterogeneous Moon. Figure 3i illustrates the uniformity of the distribution of elements from each impactor. The extreme ellipsoidal shape of the resultant Earth was a concern, but when the rotation of the Earth was slowed to a 24-hour day, the Earth became spherical. The initial parameters used for this simulation are provided in Tables 6–8.

Table 6. Parameters for planar double-tailed collision.

Parameter	Value
D	376.78 km
M_{Si}	$7.4161 \cdot 10^{19}$ kg
M_{Fe}	$1.9549 \cdot 10^{20}$ kg
K_{Si}	$7.2785 \cdot 10^{10}$kg m^{-1} s^{-2}
K_{Fe}	$2.9114 \cdot 10^{11}$kg m^{-1} s^{-2}
KRP_{Si}	0.01
KRP_{Fe}	0.02
SDP_{Si}	0.001
SDP_{Fe}	0.01
Epsilon	47.0975 km
Time step	5.8117 s
Numerical technique	Leap-frog formulas

Table 7. Initial values for planar double-tailed collision–yellow impactor.

Parameter	x value	y value	z value
Center of mass	37678.0 km	0.0 km	9042.7 km
Linear velocity	−1.29678 km s^{-1}	0.0 km s^{-1}	0.0 km s^{-1}
Angular velocity	0.0 rad h^{-1}	3.0973 rad h^{-1}	0.0 rad h^{-1}

Table 8. Initial values for planar double-tailed collision–green impactor.

Parameter	x value	y value	z value
Center of mass	−37678.0 km	0.0 km	−9042.7 km
Linear velocity	1.29678 km s^{-1}	0.0 km s^{-1}	0.0 km s^{-1}
Angular velocity	0.0 rad h^{-1}	3.0973 rad h^{-1}	0.0 rad h^{-1}

4.3 *Parallel off-planar collision*

Though it is likely that two proto-planets would be orbiting and rotating in the same direction, parallel to the ecliptic plane, it is not likely that they would both be rotating exactly in the ecliptic plane. Therefore, a more likely scenario than that depicted in the planar double-tailed collision would be of two proto-planets, both rotating and orbiting in the same direction, parallel to the ecliptic plane but not co-planar. If two such impactors collided in an off-centered collision with both impactors spinning out of the collision, a double-tailed spiral would be formed. Using the impactors' initially aligned axes of rotation as a reference for the ecliptic plane, we can measure the resultant tilt of the Earth's equatorial plane off the ecliptic plane (see Figure 4).

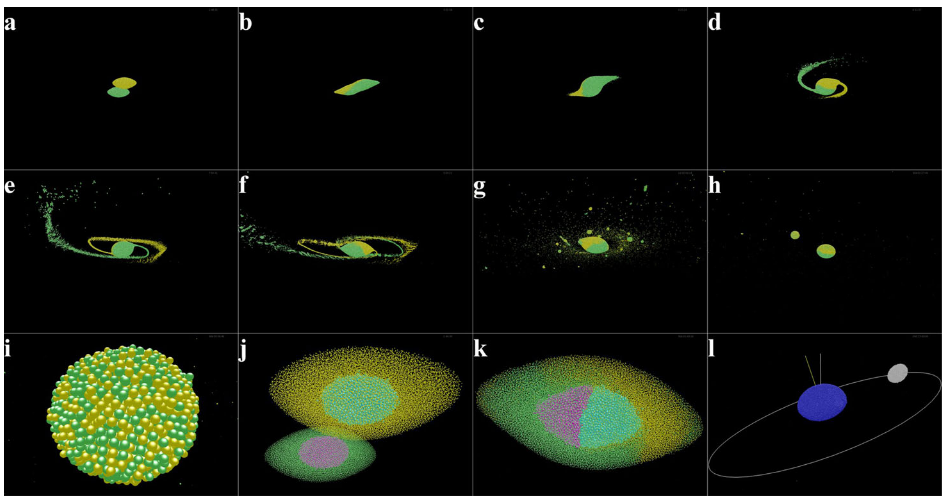

Figure 4. Parallel off-planar collision (131,072 elements). **(a–h)** Side view of collision at 2.82, 3.87, 4.42, 6.17, 7.88, 9.07, 24.00 and 720.00 hours, respectively, into the simulation. Both impactors would be spinning clockwise if viewed as in Fig. 3. **(i)** Close up of the resultant Moon. (**j**) View of impactor cores at impact. (**k**) View of the resultant Earth's core. **(l)** Trace of resultant Moon's orbit and tilt off ecliptic. The white ray is normal to the ecliptic plane, and the yellow ray is normal to Earth's equatorial plane.

Table 9. Parameters for parallel off-planar collision.

Parameter	Value
D	376.78 km
M_{Si}	$7.4161 \cdot 10^{19}$ kg
M_{Fe}	$1.9549 \cdot 10^{20}$ kg
K_{Si}	$7.2785 \cdot 10^{10}$kg m^{-1} s^{-2}
K_{Fe}	$2.9114 \cdot 10^{11}$kg m^{-1} s^{-2}
$\mathrm{KRP_{Si}}$	0.01
$\mathrm{KRP_{Fe}}$	0.02
$\mathrm{SDP_{Si}}$	0.001
$\mathrm{SDP_{Fe}}$	0.01
Epsilon	47.0975 km
Time step	5.8117 s
Numerical technique	Leap-frog formulas

Table 10. Initial values for parallel off-planar collision–yellow impactor.

Parameter	x value	y value	z value
Center of mass	24490.7 km	9042.7 km	9042.7 km
Linear velocity	-1.29664 km s^{-1}	0.0 km s^{-1}	0.0 km s^{-1}
Angular velocity	0.0 rad h^{-1}	3.0407 rad h^{-1}	0.0 rad h^{-1}

Table 11. Initial values for parallel off-planar collision–green impactor.

Parameter	x value	y value	z value
Center of mass	-24490.7 km	-9042.7 km	-9042.7 km
Linear velocity	1.29664 km s^{-1}	0.0 km s^{-1}	0.0 km s^{-1}
Angular velocity	0.0 rad h^{-1}	3.0407 rad h^{-1}	0.0 rad h^{-1}

The simulation ran for 720 simulated hours with the following results. A dominant Moon 1/26 the mass of the resultant Earth was formed. The Moon was composed predominantly of silicate material. The Moon was composed of almost equal amounts of material from each impactor, 48.7% from the yellow impactor and the remaining 51.3% from the green impactor. The Earth day was 3.39 hours. The orbital period of the Moon around the Earth was 13.88 hours. The average distance from the centre of Earth to the centre of the Moon was 36,673 km. The eccentricity of the orbit was 0.144. The resultant Earth's equatorial plane was 21.51 degrees off the ecliptic plane, only 1.89 degrees off the known value. The initial parameters used for this simulation are provided in Tables 9–11.

5. Summary and discussion

A phenomenon worth noting in each of the simulations is the kink in the spiral tails. This occurs as gravity pulls the core elements out of the base of the spiral tails. It was observed that when this kinking occurred, a stable Earth–Moon system was more likely to evolve. The kink is most pronounced in Fig. 2d. Another phenomenon that naturally occurred in many of the simulations is that the Moon formed with a rotational period that was coupled with its orbital period around the Earth. In other words, the simulations regularly produce a Moon with only one side visible from the Earth. The masses of the Moons in the presented simulations were substantially larger than the measured value of 1/81 of the Earth's mass. Numerous simulations did produce Moons with masses close to this value while preserving the properties featured in the simulations presented. We chose to present simulations that produced larger Moons because the larger size provided a more striking visual of the resultant Moon's composition. Because of the isotopic similarities between the Earth and the Moon, one of the major components of recent giant impact studies is the heterogeneous mixture of silicate material from each impactor, which we have presented here.

Having a model that readily produces stable Earth–Moon systems in one continuous simulation allows for a more holistic study of impact scenarios. In addition, the computational simplicity of the model allowed it to be effectively implemented on affordable GPUs. This enables rapid searching through the initial parameter space which includes impactor size, spin orientation, angular velocity, linear velocity, and position. Incorporating Canup's large impactor size and Cuk's large spin rates into the simulations presented here resulted in systems with excess angular momentum. This was the Royal Society's major point of debate concerning their work in the origin of the Moon meeting held in London on 2013 September 23–24 (Clery 2013). We are currently searching through the parameter space to find a giant impact that will produce both an Earth–Moon system with the proper angular momentum and a resultant Moon that is isotopically similar to the Earth. After this has been accomplished we will turn to the task of more thoroughly addressing thermodynamics in the model.

6. Methods summary

All simulations were run on a single NVIDIA 580 or 680 graphics card. The numerical algorithms were written in C, C++, and Compute Unified Device Architecture (CUDA) (Kirk & Hwu 2010). The graphical algorithms were written in C, C++ and OpenGL. The numerical schemes used were the Leap-frog formulas (Wyatt 1994) and Kutta's fourth-order formula (Greenspan 2004). Exploratory work was done with 16,384 elements and a large time step to search for promising force parameters and initial conditions. These were then used in larger simulations with smaller time steps for increased accuracy and proof of scalability. The power of the NVIDIA graphics cards allowed the exploratory work to be done in real time which was instrumental in successfully implementing the model.

Acknowledgement

The authors would like to thank NVIDIA and Mellanox Technologies for the donation of computational hardware.

References

Backman, D., Seeds, M. A. 2010, *The Solar System*, 7th ed., Boston, Cengage.
Benz, W., Slattery, W. L., Cameron, A. G. W. 1986, *Icarus*, **66**, 515.
Cameron, A. G. W., Ward, W. R. 1976, *Abstracts of the Lunar and Planetary Science Conference*, **7**, 120.
Canup, R. M., Asphaug, E. 2001, *Nature*, **412**, 708.
Canup, R. M. 2003, *Icarus*, **168**, 433.
Canup, R. M. 2012, *Science*, **338**, 1052.
Clery, D. 2013, *Science*, **342**, 183.
Cuk, M., Stewart, S. T. 2012, *Science*, **338**, 1047.
Feynman, R., Gottlieb, M., Leighton, R. 2006, *Tips on Physics*, New York, Pearson.
Greenspan, D. 2004, *n-Body Problems and Models*, Hackensack, NJ, World Scientific.
Halliday, A. N. 2012, *Science*, **338**, 1040.
Hartmann, W. K., Davis, D. R. 1975, *Icarus*, **24**, 504.
Ida, S., Canup, R. M., Stewart, G. R. 1997, *Nature*, **389**, 353.
Kirk, D. B., Hwu, W. W. 2010, *Programming Massively Parallel Processors*, Burlington, MA, Morgan Kaufmann.
Kokubo, E., Ida, S., Makino, J. 2000, *Icarus*, **148**, 419.

Meier, M. M. M. 2012, *Nature Geoscience*, **5**, 240.
Mravlak, M. 2008, *Depletion Force Seminar 3*, Slovenia, University of Ljubljana.
Newsom, H. E., Taylor, S. R. 1989, *Nature*, **338**, 29.
Palme, H. 2004, *Science*, **304**, 977.
Reufer, A., Meier, M. M. M., Benz, W., Wieler, R. 2012, *Icarus*, **221**, 296.
Ringwood, A. E. 1962, *Journal of Geophysical Research*, **67**, 4473.
Schneider, S., Arny, T. 2012, *Pathways to Astronomy*, 3rd ed., New York, McGraw-Hill.
Stevenson, D. J. 1987, *Ann. Rev. Earth Planet, Science*, **15**, 271.
Touboul, M., Kleine, T., Bourdon, B., Palme, H., Wieler, R. 2007, *Nature*, **450**, 1206.
Whipple, F. L. 1981, *Orbiting the Sun: Planets and Satellites of the Solar System*, Cambridge, MA, Harvard University Press.
Wiechert, U., Holliday, A. N., Lee, D. C., Snyder, G. A., Taylor, L. A., Rumble, D. 2001, *Science*, **294**, 345.
Wyatt, B. 1994, *Computers & Mathematics with Applications*, **28**, 175.
Zhang, J., Dauphas, N., Davis, A. M., Leya, I., Fedkin, A. 2012, *Nature Geoscience*, **5**, 251.